Journal of Mining and Environment (JME) Vol. 18, No. 4, 2026, 1389-1408

Shahrood University of Technology

Journal of Mining and Environment (JME)

Journal homepage: www.jme.shahroodut.ac.ir

Iranian Society of Mining Engineering (IRSME)

Introduction of the Fibonacci Transformation Method for Separating Geochemical Anomalous Zones on the Scale of Supplementary Explorations

Mohammadreza Agharezaei, and Ardeshir Hezarkhani*

Department of Mining Engineering, Amirkabir University of Technology (Tehran Polytechnic), Tehran, Iran

Article Info

Received 18 May 2025

Received in Revised form 17 June 2025

Accepted 18 July 2025

Published online 18 July 2025

DOI: 10.22044/jme.2025.16261.3157

Keywords

Fibonacci Transformation

Fibonacci features

Geochemical anomaly

Fibonacci index

Abstract

Geochemical exploration as an advantageous exploration method mostly deals with anomaly separation and related endeavors. Many experts have suggested various types of anomaly identification methods. The intention of this research is introduction of a new method for separating geochemical anomalies based on the Fibonacci sequence for the first time. The Fibonacci features of datasets were clarified and the method was introduced and applied on a dataset of bore-hole samples of Hired gold deposit located in southern Khorasan province, Iran. The main result of this study is the successfully establishing of a Fibonacci-based procedure that leads to separate geochemical anomalies. The determined thresholds by this method were compared with U-statistics and Concentration-Volume fractal modeling. Evaluation of the results revealed high consistence between the outcomes of the methods. The U-Statistics threshold for background was 105 ppb for gold and the Fibonacci Transformation method's threshold was 109 ppb. This new method specified 170 ppb for gold moderate anomaly and the C-V fractal determined 169 ppb which are almost the same. The performance of the new method was assessed by calculating misclassification errors. The average total misclassification error was 0.023 which is acceptable and quite reasonable since the methods are fundamentally different. As the other main results of this study, it is confirmed that one of the Fibonacci features which is defined as Fibonacci index (FI) fluctuates among element pairs in the same way that geochemical correlation does. The FI could be considered as a genetic-related factor in geochemical studies and ore evolution researches.

1.Introduction

As soon as geochemical studies began, anomaly separation has been a major discuss among experts. Efforts for determining reasonable thresholds include several scientific fields. As reported by Liu et al [1], during the past decades, several methods with various approaches have been used for identification of geochemical anomalies and separation of accurate thresholds. These methods could be categorized as univariate statistical approaches with frequency basis [2-4], multivariate procedures [5-10], and fractal/multifractal power law-based methods [11-18].

The statistical approaches have been used for decades to model different geological features and determining the spatial variables needed for evaluation of ore reserves or estimation of concentration of elements in deposits especially in unsampled parts [19-23]. Primary statistical methods applied for exploration purposes known as Exploratory Data Analysis (EDA) methods were used mainly as anomaly detection tools. The well-known methods are Box Plots [24] Probability Graphs [25] and the Mean ±2STD (Standard deviations) [26].

Multivariate procedures approaches are the next generation of geochemical anomaly detection methods used by experts. Principal Component Analysis or PCA as a robust multivariate technique, has been used for identifying

Corresponding author: ardehez@aut.ac.ir (A. Hezarkhani)

geochemical anomalies [27] and applied for mapping the anomaly of toxic metal distribution [28, 29]. The anomaly separation methods could be categorized as two main groups. Structural and non-structural methods [30]. The structural methods consider the location of the samples as a criterion to determine the anomalies while non-structural methods just consider the variable values [31]. Methods like kriging interpolation [32], trend surface [33] and U-Statistics are the most popular and applied structural approaches in geochemical studies.

Fractal/multifractal approaches introduced by Mandelbrot in 1983 [34], are capable models for anomaly detection. The dimensions defined by these models are used to separate anomalous zones and geochemical populations [35-37]. The Fractal models developed by several researches like N-S fractal (Number-Size) [34], C-A fractal (Concentration-Area) [38], C-V fractal (Concentration-Volume) [39] and the newly developed C-C fractal (concentration-concentration) [40] are used in various geoscientific fields from determining the geological variable's spatial variations to delineating geochemical anomalies [41-45]. In an innovative study, Mahdianfar et al. [46] have integrated these methods by applying fractal approach to model the principal factor of toxic elements.

The neural network-based methods generally known as a type of Machine learning (ML) methods, as new concept for processing geochemical data and anomaly detection are applied with many studies as a robust intelligent tool [47]. Generally, machine learning methods are classified as two main types; supervised and unsupervised learning methods. Unsupervised learning type is mostly employed for geochemical anomaly detection [48]. This type of neural networks is widely developed into algorithms like OCSVM (One Class Support Vector Machine) [49], DAE (Deep Auto Encoder [50, 51], graph attention networks [52], and GAN (Generative Adversarial Networks [53]. A superiority of Machine learning methods to the statistical approaches is that ML methods do not require that variables to have specific distribution like normal distribution [54].

The methods mentioned above are mostly based on statistical approaches. In other words, these methods treat the geochemical datasets equally like a dataset generated with a machine randomly, and without considering their natural features. One of these natural features is Fibonacci characteristic of geochemical datasets that has been introduced for the first time through this paper. In this study a new concept of dataset's essence is introduced; the Fibonacci features of a dataset. While all of the present methods do not care about the dataset origin and their intrinsic features, Fibonacci Transformation method lights on the hidden features of datasets and is capable of discovering deep level relations between variables. The Fibonacci sequence has been used previously in geophysics to develop a seismic ray-tracing method [55]. The tracing method was based on the Fibonacci search algorithm which is a comparison-based search technique. The approach presented in our study is not an application of an already existing method/algorithm but this is an introduction of a new concept for datamining the geochemical datasets based on the Fibonacci ratios. Using this new method, geochemical populations could be separated. The method uses Fibonacci features of datasets to separate anomalies. This method, like ML methods, does not necessitate that the variables belong to any specific distribution. A case study was investigated to demonstrate its application potential. The accuracy of this method was tested by comparison to previously mentioned method's results, U-statistics and C-V fractal modeling for the same case study.

2. Methodology

2.1 Fibonacci Transformation method

2.1.1 Fibonacci sequence

The Fibonacci numbers, derived their name from the Leonardo of Pisa lived in 1202 known as Fibonacci. These numbers (the Fibonacci sequence) were introduced in his book, Liber abaci, for the first time [56, 57]. By defining $F_n = F_{n-1} + F_{n-2}$, the Fibonacci sequence could be generated for different values of n. Based on the introduction of the sequence, the n values must be integer numbers greater than 1 [58]. To avoid possible confusion, the numbers in the Fibonacci sequence are called briefly "Fibonacci numbers" in this manuscript. Dividing F_n by F_{n-1} results in a constant number called the golden ratio ($\phi=\frac{1+\sqrt{5}}{2} \simeq 1.618$). N.Menhinick [59] has published the book: 'The Fibonacci Resonance and Other New Golden Ratio Discoveries' in which occurrences of Fibonacci numbers and the ratio among them (the golden ratio) in nature, music, art and architecture is introduced to the readers. The Fibonacci sequence is known to even non mathematicians too [60]. The relation between Fibonacci numbers is not limited only to the golden ratio. Dividing a

Fibonacci number to the previous/next second, third and so on numbers will also result in constant ratios too (just only not in a few cases). Table 1 depicts some of these ratios among Fibonacci numbers. The numbers of these ratios are infinite and are accessible by dividing a Fibonacci number by the previous or next numbers in the sequence. The Fibo-ratio of 0.768 is an unusual Fibo-ratio among other ratios. The origin of this ratio is not very clear in the literature. The actual result of the square root of $\frac{F_{n-1}}{F_n}$ is 0.786 but the Fibo-ratio used in literature is 0.768.

Table 1. Constant Ratios between Fibonacci numbers

Ratio equation	$\frac{F_{n-1}}{F_n}$	$\sqrt{\frac{F_{n-1}}{F_n}}$	$\frac{F_{n-2}}{F_n}$	$\frac{F_{n-3}}{F_n}$
Ratio value	0.618	0.768	0.382	0.236

Fibonacci numbers have been studied by mathematicians from different points of view. Most of the studies cover "number theory" field. The sequence has been studied by several researchers and as a result new sequences based on the Fibonacci sequence have been established [61]. These studies reported by Cheddour et al. [61] are as below:

Introduction and study of Klippel-Feil syndrome or K FS by Falcon and Plaza [62] followed by an endeavor of Edson and Yayenie [63] in studying FS. Their research resulted in generalizing and proving some related identities of FS. Wall [64] started the study of algebraic structures with the view point of recurrence sequences in them by determining regular FS in cyclic groups. Afterward, the concept of the theory lead to linear recurrence sequences developed by other researchers. As an example, the theory was developed to the quaternions by Deveci and Shannon [65].

The study of Fibonacci sequence is mostly limited to the mentioned subjects and there is no scientific use of these numbers in geosciences and related fields. This research is the first study that applied Fibonacci numbers for aiming geoscientific purposes.

2.1.2 Fibonacci sequence in nature

Fibonacci numbers and ratios are observed in nature for several times. In plants, Fibonacci numbers are seen frequently. As an illustration, the numbers of petals in many flowers or the number of florets spirals in a sunflower are Fibonacci numbers (Figure 1). Not only the Fibonacci numbers are observed but also the golden ratio among plants parts is measured too. The golden ratio of typical leaves demonstrated as Figure 2. These observations are not limited to these examples and include various plants types. Besides, the ratios of human body parts in many cases are also Fibonacci ratios. As another example, the length of forearm to palm length ratio is 1.618 (the golden ratio) (Figure 3).

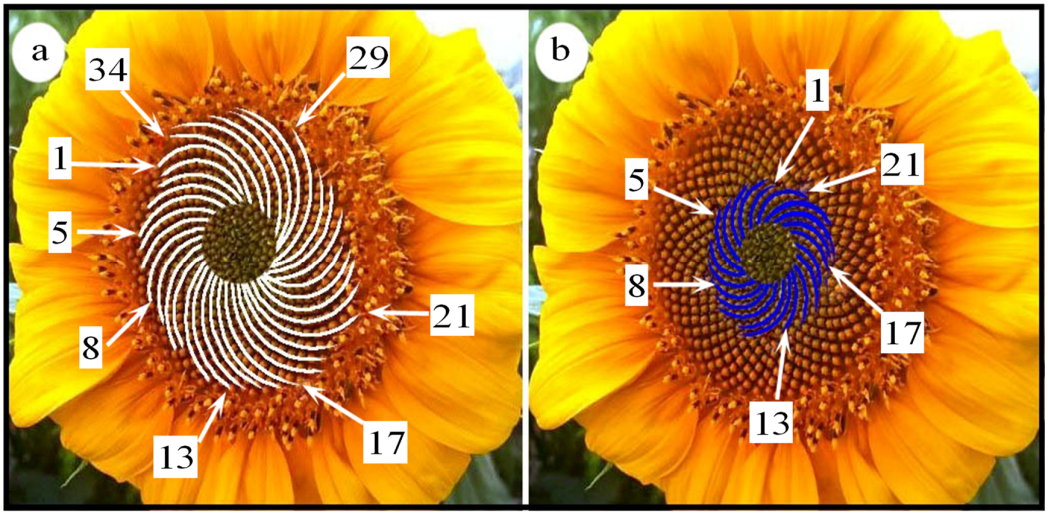


Figure 1. Florets spirals in sunflower, a) 34 left-handed spirals and b) 21 right-handed spirals

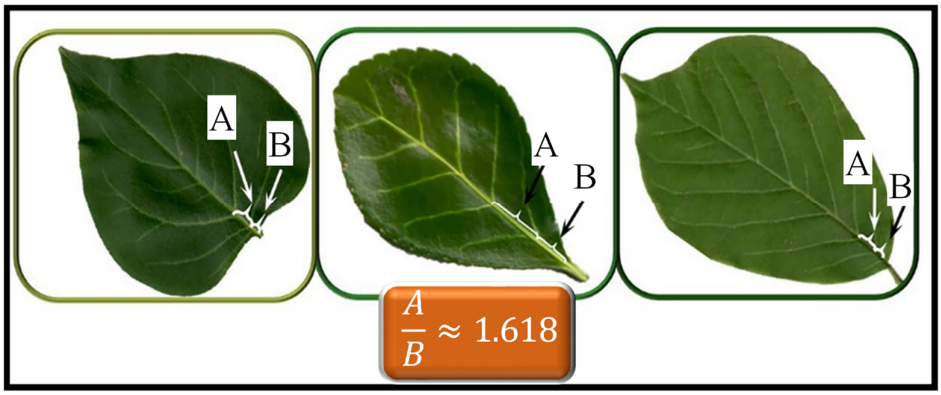


Figure 2. Golden ratio in typical leaves (modified after Sun et al) [66]

Anyone studying Fibonacci numbers is familiar with Fibonacci spiral too. This spiral is created by assuming each Fibonacci number as sides of squares. By linking the corners of each square oppositely, the spiral will be the made (Figure 4). Fibonacci spiral is a type of logarithmic spirals. This spiral also known as golden spiral is a fundamental basis in phyllotaxis (the pattern or arrangement of leaves on the stem or branch of a plant) studies. If botanical elements are repeatedly produced at leaves, bractae and florets of a vascular plant, the result would be patterns which are called phyllotaxis. Based on the observation of these patterns, the impressive feature of this type of patterns is in their accordance to the Fibonacci sequence [67]. There are much more fingerprints of Fibonacci numbers in nature. Since geochemical processes are also natural phenomenon, the idea of using Fibonacci numbers for studying these data is suggested by this study for the first time.

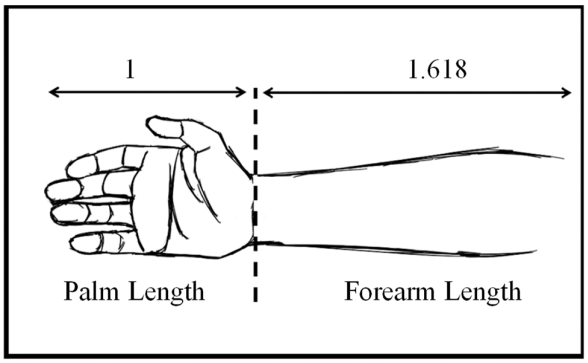


Figure 3. Fibonacci Golden ratio in human's body parts

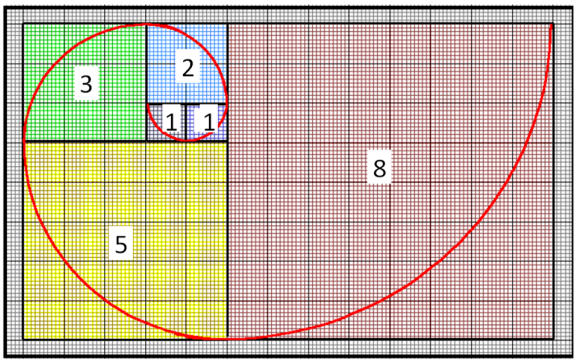


Figure 4. Fibonacci spiral

2.1.3 Fibonacci Transformation theory and applications

2.1.3.1 Theory and concepts

Geochemical data are obtained from nature. Based on various observations of Fibonacci numbers in nature, we aim for uncovering Fibonacci features behind geochemical datasets. Mineralization as a natural process may also follow the same rules that resulted in Fibonacci behavior of other natural procedures. In Fibonacci transformation method, the Fibonacci features of geochemical datasets are examined. Geochemical datasets mostly consisted of multi-element analysis. These datasets are usually studied statistically because of their numerical nature. In this study we suggest that a geochemical dataset could have Fibonacci features among its components. Since the single or multi-elemental analysis of a sample (surface or borehole sample) measures a quantity formed in nature, it is possible to expect Fibonacci relations and ratios among the constituent members of this kind of dataset.

2.1.3.2. Data pre-processing

Pre-processing geochemical data is a vital step in any numeric study related to this type of dataset. Geochemical datamining including statistical frequency-based approaches to power-law models involve numerical studies of the dataset. Using quantitative data is also needed for studying

Fibonacci features. The geochemical datasets are derived from several analytical techniques like Inductively Coupled Plasma Optical Emission spectroscopy (ICP-OES) and other analytical methods. The data are reported as sheets of multi-elemental analysis for each sample. This is called raw data. Statistical methods require normal distribution of datasets. Known distribution model of dataset makes it easier to outline geochemical anomalies [68, 69]. In cases of abnormality, geochemists normalize datasets with statistical tools because using standard statistical methods for studying abnormally-distributed populations leads to indefinite models and incorrect interpretations [70]. In order to standardize/normalize data in Fibonacci transformation method we used the famous Z-score method using average and standard deviation as following equation:

$$Z = \frac{X_i - \mu}{\sigma} \quad (1)$$

Where the sample index is i, the variable value is X, the normalized form of X is Z, μ and σ are the average and the standard deviation of the intended variable respectively. This procedure rescales dataset and arranges datapoints around an average of 0 and a standard deviation of 1. It is better to name Z-Score as a standardizing method rather than normalizing tool since the procedure does not change the distribution (histogram) of the numeric data.

The other challenge in geochemical datamining is outlier's effect. Outliers affect the modeling and interpretation of geochemical datasets [71]. Median is a useful tool for studying a statistical population. Statistics of median can be applied for several applications and computations [35]. As an example, median was used by Gott and Turner [73] for calculating mass-to-light ratios among groups of galaxies to decrease the outlier's (background and foreground) effects. Median as one of the central tendency measures is not affected by outliers unlike mean. In Fibonacci transformation method we used median as a robust statistical tool for studying geochemical datasets.

2.1.3.3. Method application steps

According to the name of this method, a transformation plays the role. With this transformation, datapoints are changed into new datapoints by applying Fibonacci ratios to the median of the dataset. Using median of a variable as the representative of the population facilitates precisely data modeling. The steps of Fibonacci Transformation method are clarified as bellow:

1) Calculate median of raw data and multiply it by Fibonacci ratios (Fibo-ratios). Continue this process until the resulted values follow these relations:

   minimum datapoint ≤ Median*Fibo-ratios
   maximum datapoint ≥ Median*Fibo-ratios

2) Calculate average and standard deviation of values in step1. Let's call them FibAve and FibStdev respectively.
3) Standardize raw data based on equation (1).
4) Change standardized data in step 3 back to raw data by using FibAve and FibStdev instead of the raw data average and standard deviation (now Fibo-Transformed data are created).
5) Calculate Range (R) of the Fibo-Transformed data as: R= max-min.
6) Multiply R by Fibo-ratios. Call them ranges
7) Select the ranges which are greater than the min (Fibo-Transformed data) and smaller than max (Fibo-Transformed data).
8) Add min (Fibo-Transformed data) to values in step 7. Call them interval numbers.
9) Consider min (Fibo-Transformed data) and max (Fibo-Transformed data) as interval numbers list too.
10) Sort interval numbers from low to high. Each pair of the consecutive numbers is an interval range.
11) Calculate cumulative sum of the variable values for each interval range.
12) Draw the diagram of cumulative values of variable versus interval ranges.
13) Breakpoints of the diagram are the thresholds that separate geochemical populations. The breakpoints values must be transformed back to their initial values to achieve real thresholds because the diagram shows transformed concentrations of the element. This step is similar to anti-logarithm operation in the case of using logarithmic transformation.

Figure 5 depicts the flowchart of the above steps to better illustrate the process. To facilitate the application of the method, the algorithm code of the method with MATLAB syntax has been presented by the authors too (Figure 6).

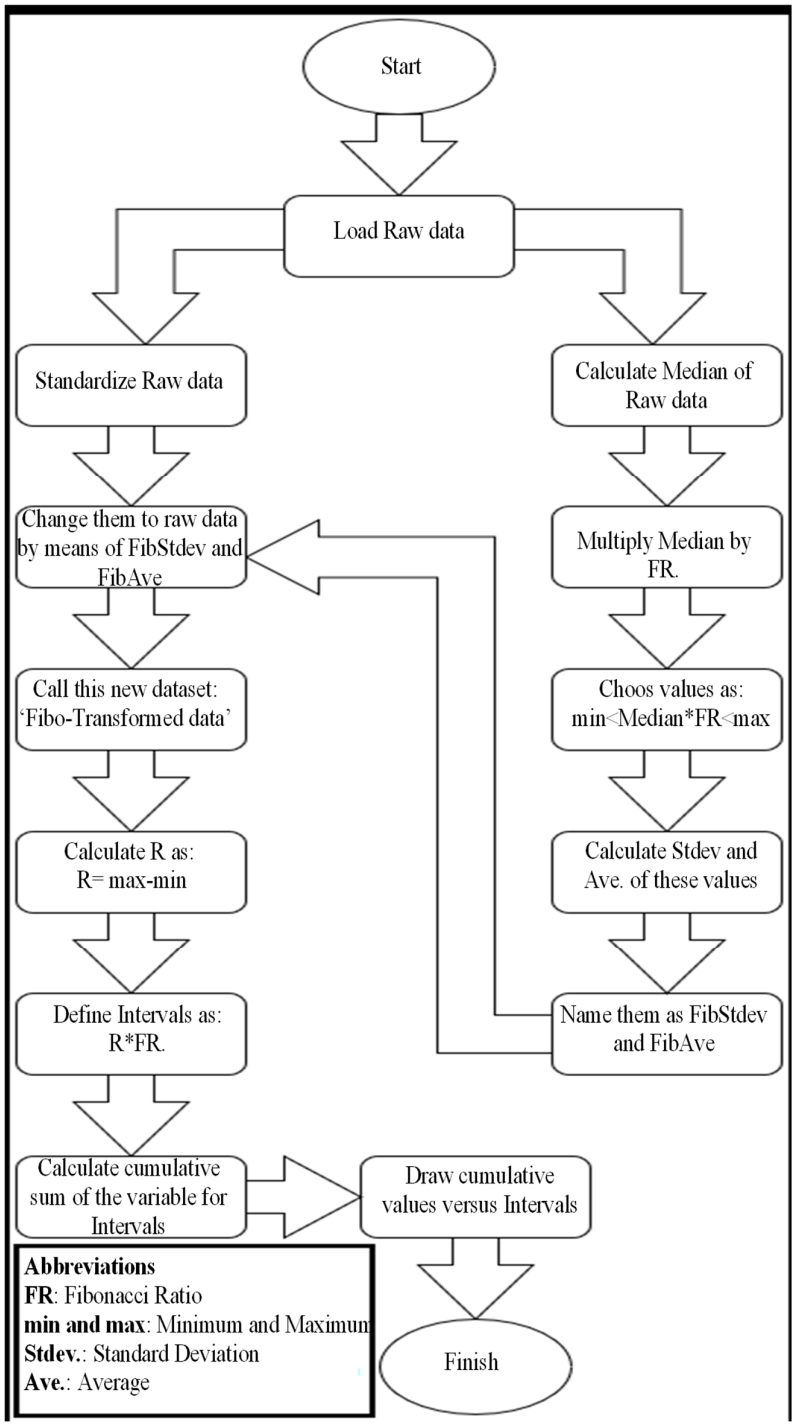


Figure 5. Flowchart of the Fibonacci Transformation method

```
function results = fibo_data_mining(raw_data)
% FIBO_DATA_MINING Performs Fibonacci ratio based data mining steps on raw_data.
% This version uses a predefined list of Fibonacci ratios and implements
% the interval generation (Steps 8-11) and cumulative sum (Step 12) as
% precisely specified in the latest request.
 %
 % Input:
 %   raw_data - numeric vector of raw data. Can be a row or column vector.
 %
% Output:
 %   results - struct containing all intermediate results and final outputs.

% Ensure raw_data is a row vector for consistent operations
raw_data = raw_data(:)';

% Input validation
if isempty(raw_data)
error('FIBO_DATA_MINING:EmptyInput', 'Input raw_data cannot be empty.');
end
if length(raw_data) < 2
warning('FIBO_DATA_MINING:SmallData', 'Raw data has less than 2 points. Some
calculations (like std dev) might be trivial or undefined.');
end

disp('--- Starting Data Mining Process ---');
disp(['Raw Data: ', mat2str(raw_data)]);

% Step 1: Calculate Median of raw data
med_raw = median(raw_data);
disp(sprintf('\nStep 1: Median of Raw Data: %.4f', med_raw));
```

Figure 6. The algorithm code of Fibonacci Transformation method with MATLAB syntax

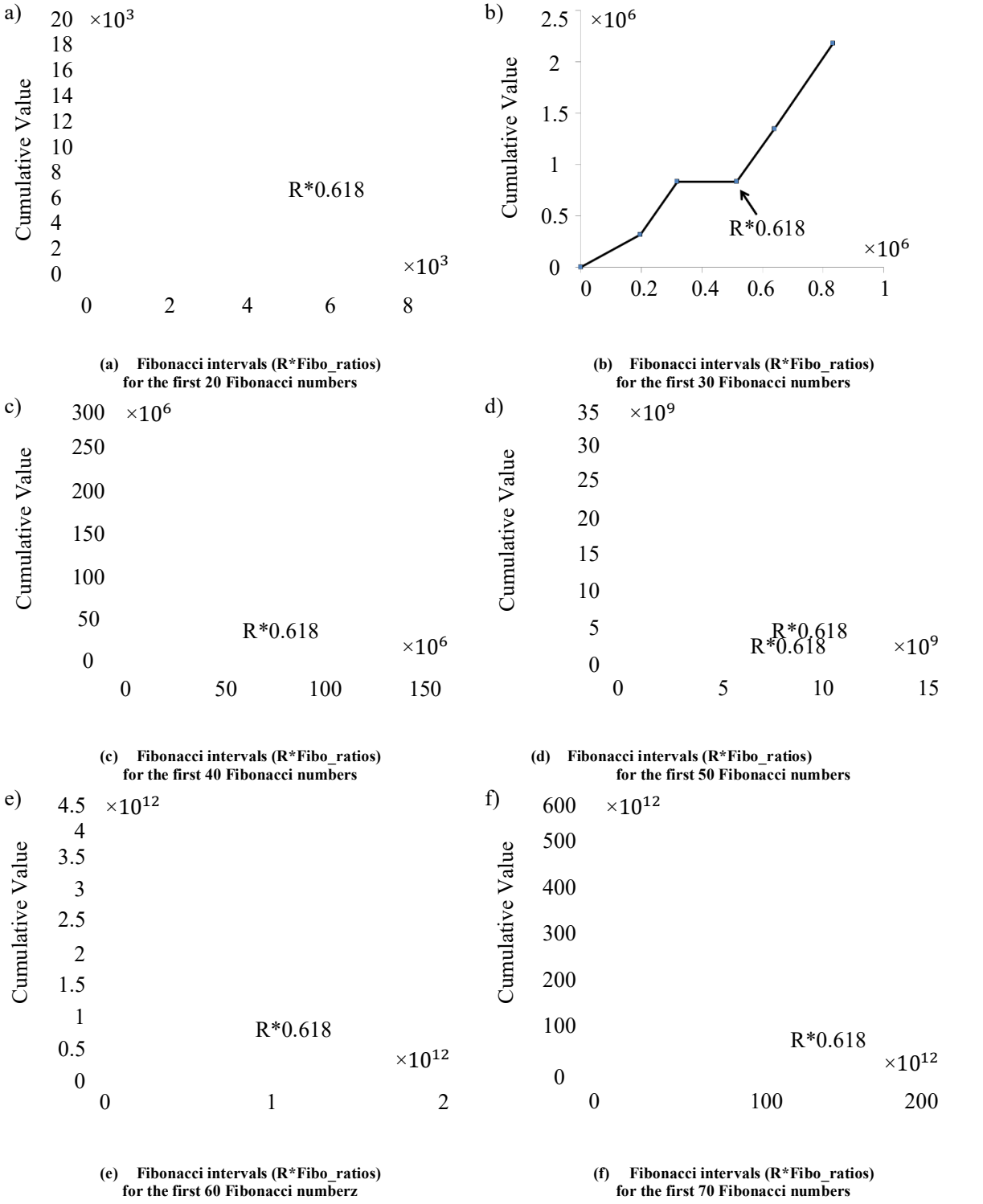
The complete code has been uploaded as a MATLAB m-file on an online repository. The file download link is available in appendix section. The use of the code is very simple. Users should copy the whole code or save the m-file in a folder and name it as 'fibo_data_mining' and the input data should be defined as 'raw_data'. The outcome of the algorithm is the diagram explained in step 12.

2.1.3.4. Fibonacci features of a dataset

This method was introduced to depict the Fibonacci features of datasets and delineate anomalies. By assuming the Fibonacci sequence, itself as a dataset, the Transformation method was firstly applied for the sequence. In this case, we have assumed that for example the Fibonacci sequence itself is a geochemical dataset and the numbers of the sequence are the measurement of concentrations of a geochemical element. Figure 7 shows the outcome of the Fibonacci Transformation method (diagram of step 12) for different numbers of the sequence. Based on figure 7a to 7f, for different numbers of the Fibonacci sequence members, the same pattern is obtained by drawing cumulative sum of Fibonacci numbers versus intervals defined by Fibonacci Transformation method. For different numbers, same breakpoints are observed which could be interpreted as the thresholds. By passing the specified point on the diagrams (point R*0.618) the cumulative value increases drastically which is indicating anomaly threshold. Since the shape of the diagrams are similar and constant, we called them reference diagrams. It could be considered as the first Fibonacci feature meaning that in studying other datasets, as long as the diagram is similar to the reference diagrams, the Fibonacci feature of the datasets is proved and the more similarity means the more Fibonacci characteristic of the dataset.

By transforming dataset through Fibonacci Transformation method, the new datapoints achieve more continuity if and only if the raw dataset is convergent to the values generated in step 1 of the method. If the raw dataset is not convergent to the values in step 1 then the method is not applicable for the dataset because of the lack of Fibonacci feature in the raw data. Since Median*Fibo-ratios values comprise Fibonacci property intrinsically, continuity increase among Fibo-Transformed datapoints manifests another Fibonacci characteristic of the raw dataset. Continuity increase could be defined as decrease of standard deviation of dataset. By considering the Fibonacci sequence from this aspect, it is revealed that standard deviation decreases when Fibonacci Transformation method is applied to the sequence. Figure 6 depicts the division of Standard deviation of Fibo-Transformed data

(FibStdev) by the standard deviation of raw data (Fibonacci sequence members). To summarize we named the fraction ($\frac{\text{FibStdev}}{\text{Stdev}}$) as Fibonacci index (FI). The downward trend demonstrates that standard deviation decreases when data are transformed via Fibonacci Transformation method.



(a) Fibonacci intervals (R*Fibo_ratios) for the first 20 Fibonacci numbers

(b) Fibonacci intervals (R*Fibo_ratios) for the first 30 Fibonacci numbers

(c) Fibonacci intervals (R*Fibo_ratios) for the first 40 Fibonacci numbers

(d) Fibonacci intervals (R*Fibo_ratios) for the first 50 Fibonacci numbers

(e) Fibonacci intervals (R*Fibo_ratios) for the first 60 Fibonacci numberz

(f) Fibonacci intervals (R*Fibo_ratios) for the first 70 Fibonacci numbers

Figure 7. Fibonacci Transformation method results for the Fibonacci sequence

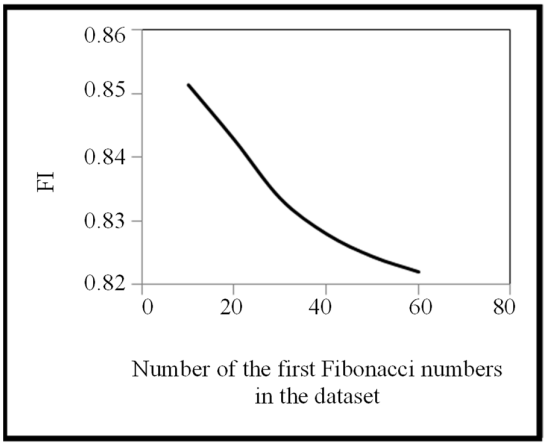


Figure 8. FI (division of standard deviation of Fibo-Transformed data (Fibstdev) by raw data standard deviation) versus number of the first Fibonacci numbers

As proved by figure 8, standard deviation of the Fibonacci sequence as a dataset that possess the most Fibonacci features, decreases after applying Fibonacci Transformation method. It is worth repeating that in this case we have assumed the Fibonacci sequence numbers as a geochemical dataset meaning that we have treated the numbers in the sequence (0, 1, 1, 2, 3, 5, 8, ...) for example as an element's concentration values and we have applied the Fibonacci Transformation method to study this dataset. The decrease of standard deviation of Fibo-Transformed data could be named as 'the second Fibonacci feature'. As we have proved mathematically (Figure 8), any phenomena in the nature that has the Fibonacci characteristics must react similarly the same way as the Fibonacci numbers reacted under the Fibonacci Transformation method and this is because the Fibonacci sequence numbers have the highest Fibonacci characteristics between them. According to this feature, the relation between Stdev and FibStdev of a dataset with Fibonacci feature is Stdev ≥ FibStdev and FI = $\frac{\text{FibStdev}}{\text{Stdev}}$ so FI ≤ 1.

Datasets with these two features are highly corelated with Fibonacci sequence's essence so they are eligible to be considered as datasets that have Fibonacci features.

2.2. U-statistics method

The U-statistics is a spatial anomaly separation method used for separating geochemical anomalies by employing a running average with a changeable search radius [74]. For a certain point (i-th point) and a search radius 'r', different values for U are calculated based on the equation (2). Each sample inside the search windows is weighted based on the distance between the sample and the target point (i-th point). By weighting the samples, the dispersion of samples is calculated.

$$U_i(r) = \frac{\overline{x}_i(r) - \mu}{\sigma} \quad (2)$$

in which r is the search radius and $U_i(r)$ is a function of radius, μ is average and σ is standard deviation of the dataset respectively. $\overline{x}_i(r)$ contains the sum of the multiplication of each point's value by the allocated weight to the point defined as equation (3):

$$\overline{x}_i(r) = \sum_{j=1}^{n} w_j(r) * x_j \quad (3)$$

in which $w_j(r)$ is the weight of point with index 'j' and x_j is the variable value of the point. By calculating U values for $0 \le r \le r_{max}$ for each point, the U value assigned to the point will be the maximum one among the calculated U values for the intended point.

The U-statistics approach has been widely used for separating anomalous samples from background [30]. Innovative studies have integrated U-statistics with other known methods. To illustrate, the study done by Ghavami et al. [75] has modeled U-statistics data on a probability plot to recognize geological features of the study area/location and the effective parameters on the concentration of the target elements. Seyedrahimi-Niaraq [76] has compared U-statistics with Classical statistics to delineate geochemical anomalies. The other innovative use of U-statistics is the work done by Ghannadpour and Hezarkhani [77]. They used U-statistics to study three dimensional datasets (borehole data). We have used their approach in this research because our dataset was obtained from bore-hole samples. The hypothesis of the 3D form is the same as the original U-statistics approach. The dissimilarity is in calculation volume which is tripled in 3-dimensional mode. Since the ordinary 2-dimensional U-statistics delineates surface anomalies, the 3-dimensional form distinguishes anomalous points from background spatially. Using the 3D form could be very informative if it is combined with geological and structural interpretations.

2.3. Concentration volume fractal

Concentration volume (C-V) fractal modeling as expressed by Afzal et al. [39] was introduced by the developers of the method as:

$V(\rho \le v) \propto \rho^{-a1}$; $V(\rho \ge v) \propto \rho^{-a2}$

Where V for $\rho \le \upsilon$ and $\rho \ge \upsilon$ are the volume values enclosed by the contour value ρ, υ is the specified threshold considered as a criterion for volume calculation and characteristic exponents are represented as a1 and a2.

By plotting a log-log diagram for the concentration of the variable versus the volume, some breakpoints appear. The concentration of the variable related to the breakpoints are the thresholds that separate different geochemical populations. The accurate calculations will result in thresholds that are in high consistency with the geological conditions of the case study [78].

3. Case study, Results and Discussion

The case study in this research is Hired gold deposit located in Khusf county, southern Khorasan province, Iran. Detailed exploration in this site includes borehole drilling and sampling for better understanding of the deposit conditions and features. The dataset used in this study is being used for a scientific purpose for the first time. In this section geological settings and dataset were reviewed and the Fibonacci Transformation method was applied to separate gold geochemical anomalies.

3.1. Geological settings

The case study in this research is Hired deposit. This gold deposit is located in eastern part of the Lut block and beside the Sistan suture zone. This structural zone with north-south trending is the result of closure of oceanic basin (strip) between the Lut and the Afghan block at the end of Mesozoic [79]. Most of the recognized metallic deposits in the area are hydrothermal vein type deposits [80]. In this deposit type, the structural situation of the area controls deposit forming processes that results in the spatial consistence of the deposits to the structural features [81-84].

In Hired gold deposit five major rock unites are detected as demonstrated in the geological map of the deposit (Figure 9). These unites are: 1) Crystal and lithic andesitic tuff (E^{lf}), 2) Ignembrite and vitric tuff (E^{i}), 3) Altered basaltic andesite (E^{ab}), 4) Young Terraces (Q^{t}), and 5) Recent alluvium (Q^{al}). According to the map, an intrusive mass ("m" abreviation in map) with granitic composition exists in northern part of the deposit (red colored). Mineralization in Hired deposit took place in silicified, carbonated and argillic fault zones as silicified-carbonated veins with variable thickness and fluctuating gold concentrations. Mineralization in surficial parts is so extremely oxidized that pyrite and arsenopyrite minerals are being altered to Iron oxides and hydroxides. The intensity of oxidation decreases by depth increase.

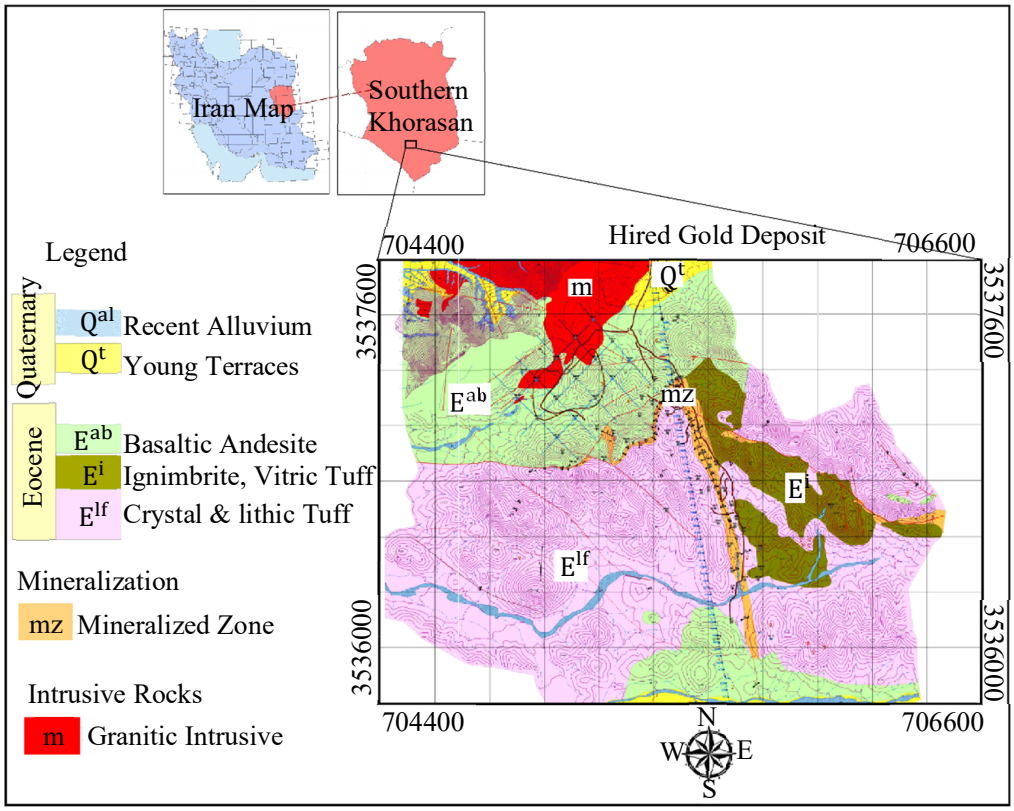


Figure 9. Simplified Hired gold deposit geological map

3.2 Sampling and Dataset

In order to achieve detailed exploration goals, borehole drilling was done. By drilling 15 boreholes with over 3000 meters of total drilling depth, 498 samples were obtained by 1.5 to 3 meters sampling intervals. The samples were analyzed by Zarazma laboratory by means of inductively coupled plasma optical emission spectroscopy (ICP-OES) method for not only gold but also 10 other elements. For gold, fire assay technique was used as a preparing analysis step. Thompson and Howarth [85] method was used as an estimation for analytical precision. Based on this method, most of the samples for different variables (analyzed elements) are under the 10% line which indicates high accuracy of the analysis processes.

3.3 Anomaly separation results and discussion

3.3.1 Fibonacci transformation method for geochemical anomaly separation

Gold (Au) as the target element was studied by this method. Fibonacci Transformation method steps were employed for gold as described in section 2.3.3. The results were compared with U-statistics and concentration volume fractal to see how precisely Fibonacci Transformation method has delineated anomalies. To avoid possible confusion, the method is employed step by step in this section.

Step 1:

Based on the dataset used in this study, median for Au was 14.285 ppb. This median was multiplied by Fibonacci ratios. The results are shown in table 2. Different Fibonacci ratios were employed based on not to break or exceed the minimum and maximum gold concentrations which were 3.75 and 437 ppb respectively. The red rows in the table 2 are invalid values because the results fall outside the max and lower than min raw data point.

Step 2:

The average and standard deviation of the result of table.2 (Fibo-ratios*Median) are 107.36 ppb and 134.55 ppb respectively. In order to avoid confusion, the former was renamed as “FibAve” and the latter as “FibStdev”.

Step 3 and 4:

The primary raw dataset was standardized by equation (1) and turned back to new raw data by FibAve and FibStdev. The new raw dataset is a transformed dataset and named as “Fibo-Transformed data”. The primary raw data average and standard deviation were 86.053 ppb and 136.775 ppb, respectively. By comparing them to FibAve and FibStdev, it can be inferred that the dataset already has the second Fibonacci feature (Standard deviation ≥ FibStdev or FI ≤ 1). Checking this condition is vital and in the cases that this condition does not apply, the Fibonacci Transformation method should not be used because the dataset does not have Fibonacci features.

Table 2. Au median multiplied by Fibonacci ratios results

Fibonacci ratios (Fibo-ratios)	0.236	0.382	0.618	0.768	1.618	2.618	4.236	6.854	11.090	17.944	29.034	46.979
Fibo-ratio*Median	3.37	5.46	8.83	10.97	23.11	37.40	60.51	97.91	158.42	256.33	414.75	671.10

Step 5:

The minimum and maximum data among Fibo-Transformed data are 26.40068 and 452.6227, respectively. So, the R value (defined as R= max – min) would be R=426.2220.

Step 6 to 11:

In this step, cumulative sum of the values for Au in Fibo-Transformed data were calculated for R*Fibo-ratios intervals. The results are shown in table 3. Since R is defined as R=max-min, the minimum data point (min) must be added to the result of multiplication of R by Fibo-ratios. Note that the min and max points are also considered as Interval numbers. The R value is calculated in Cartesian coordinate system with [0,0] origin but the origin of our calculation is not 0. The origin is the min point. So, to keep [0,0] as the origin of the coordinate system, the min value must be added to the interval numbers.

Table 3. Cumulative values of Au

Fibo-ratios	Intervals (R*Fibo-ratios)	Cumulative value
	452.6227 (max)	53469.71
0.768	353.739	27444.79
0.618	289.806	24230.53
0.382	189.217	20038
0.236	126.989	15937.28
	26.40068 (min)	2006.451

Step 12 and 13:

The diagram of cumulative values of Au versus the intervals (table 3) was drawn (Figure 10). The breakpoints of the diagram are thresholds of the different populations as explained in section 2.3.3. The diagram and the values of the breakpoints are Fibo-Transformed data. So, the values should be transformed backward to their initial form by standardizing them with FibAve and FibStdev and then the standardized values should be changed to primary raw data by using average and standard deviation of the primary raw data. The breakpoints in the diagram (Figure 10) are the different thresholds for separating anomaly. Based on the result of Fibonacci transformation method, anomaly from background is separated at 130 ppb of gold. This value is a Fibo-Transformed value and must be transformed backward to its equivalent in raw dataset. To reach the threshold value (non Fibo-Transformed), the value is firstly standardized by equation 1 using gold FibAve (107.369) and FidStdev (134.556). Then the standardized value is multiplied by Standard deviation of raw data (136.775) and the average of raw data (86.053) was added and resulted in 109 ppb as background threshold. This procedure changes Fibo-Transformed data back to their raw form. The same procedure is applied for Moderate and strong anomalies thresholds and resulted in 170 ppb and 335 ppb of gold for the mentioned thresholds respectively.

Drawing raw data and Fibo-Transformed data versus the intervals defined by the method (Figure 11) clarifies how Fibo-Transformation method rescales data points. Based on figure 11, the Fibo-Transformed data are more similar to the reference diagrams (Figure 7). This diagram could be used to evaluate the first defined Fibonacci feature too. It would be a descriptive evaluation like when normality of a histogram is compared to the bell-shaped pattern. In other words, the Fibo-Transformed data series in figure 11 are more similar to the reference diagrams (Figure 7) than the raw data series. The more similarity between the reference diagrams and the diagram of Fibo-Transformed data versus cumulative sum of the variable shows that the dataset has higher levels of Fibonacci features.

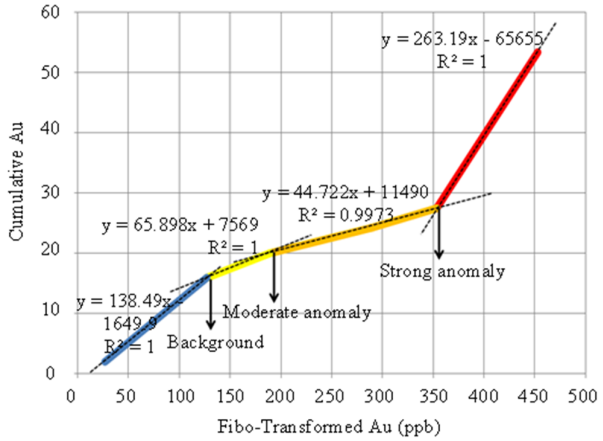


Figure 10. The diagram of cumulative values of Au versus the intervals

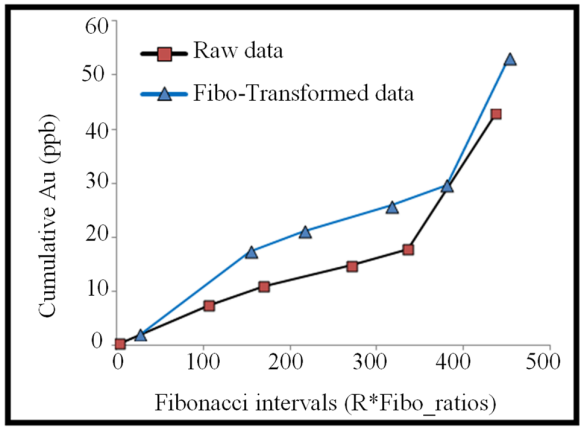


Figure 11. Raw data versus Fibo-Transformed data

3.3.2. U-statistics method

As a way to separate gold anomalies by means of U-statistics method, radius and its increase rate must be set. In this study, the initial radius was selected as the minimum sampling distance (1.5m) with an increase rate of 1 meter. U values for all samples were calculated by 3D U-statistics method and frequency distribution for U values was plotted (Figure 12). $\overline{U} = 0$ was selected for detecting background threshold. Probable and absolute anomalies were separated using $\overline{U} + 2S$ and $\overline{U} + 3S$ respectively. Based on the $\overline{U}$ and S values, 105, 193 and 320 ppb were defined as background, probable and absolute anomalies thresholds for gold respectively.

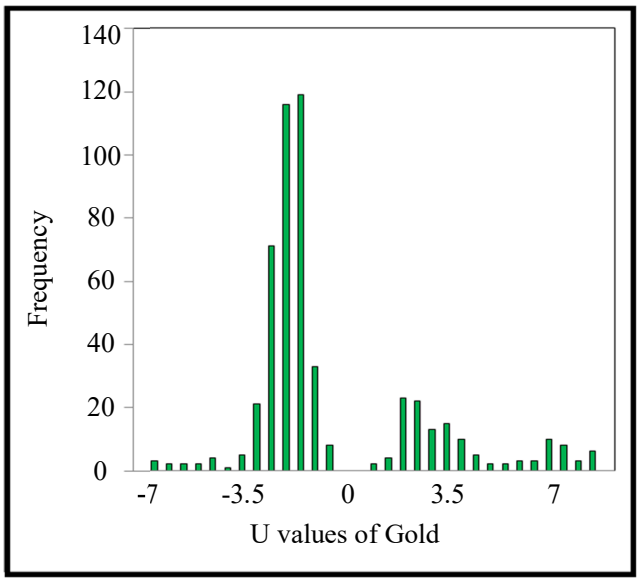


Figure 12. Frequency distribution graph of U values for gold

3.3.3 Concentration volume fractal

To better understand the accuracy of the method, the results were compared with concentration volume fractal too. The volume calculation for different grades is essential for C-V fractal modeling. In this study Rockworks 14 software was employed for 3D block modeling and volume calculations. After volume calculation, log-log plot of volume versus Au was drawn as figure 13.

Fibonacci Transformation method suggests 109, 170 and 337 ppb of gold (figure 8 breakpoints) as thresholds for separating background, moderate and strong anomalies respectively. U-statistics method is a structural approach for delineating anomalies meaning that the locations of samples directly affect the results. The outcome of U-statistics method revealed that 105, 193 and 320 ppb are the background, moderate and strong anomalies respectively. The C-V fractal modeling results are 87, 169 and 288 ppb for the mentioned thresholds.

For making a better comparison between the methods, 3D model (deposit shape) is provided (Figure.14) and misclassification error for separation of background, moderate and strong anomalies are estimated. The 3D model is created with RockWorks/14 software. Figure14-A is the deposit shape resulted from the Fibonacci Transformation method. Figure14-B and Figure14-C are the deposit shape based on U-Statistics and C-V fractal methods respectively. These models depict the recognized anomalous blocks (deposit shape) from background by each method. Based on figure 14A to C, the Fibonacci Transformation method has detected the background threshold and the ore shape almost the same as U-statistic did. These 3D models are created based on the background thresholds defined by the methods.

The misclassification errors are calculated based on the statements bellow [77]:

$$e_1 = \frac{\text{number of samples from anomaly classified as background}}{\text{total number of samples in anomaly}}$$

And

$$e_2 = \frac{\text{number of samples from background classified as anomaly}}{\text{total number of samples in background}}$$

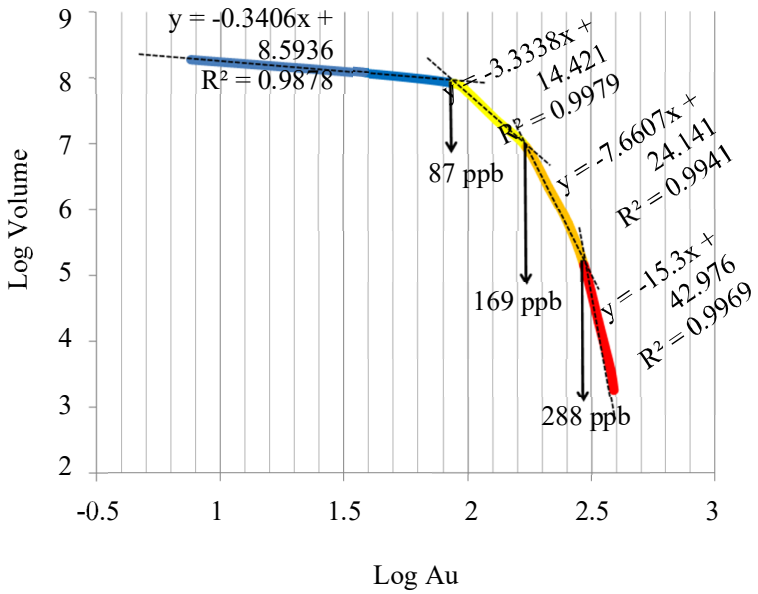
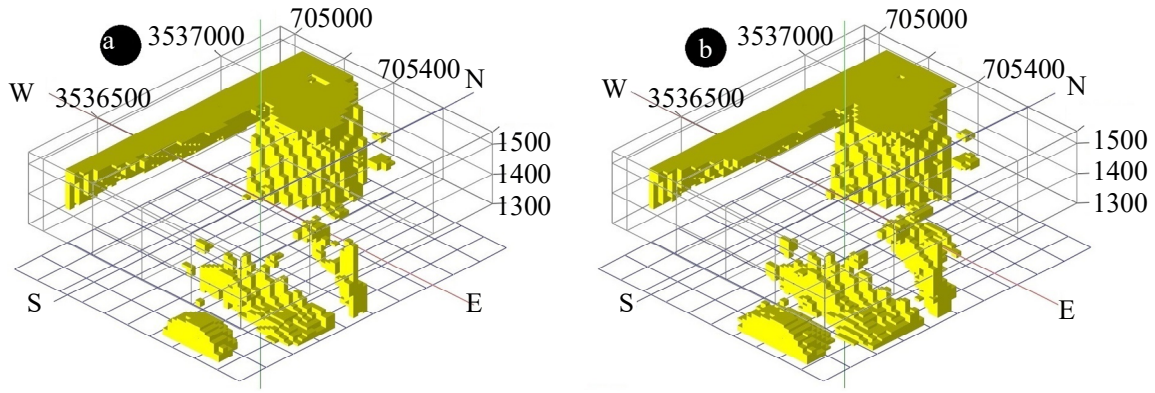
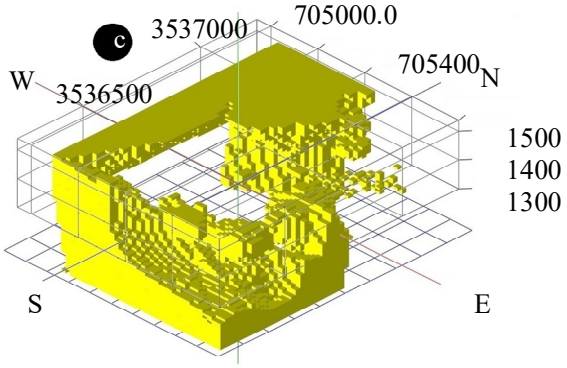


Figure 13. Concentration-Volume log-log plot



(a) Deposit shape based on the Fibonacci Transformation method

(b) Deposit shape based on the U-Statistics



(c) Deposit shape based on the C-V fractal

Figure 14. Deposit shape based on the Fibonacci Transformation method (A), U-Statistics (B) and C-V fractal (C)

These statements are frequently used for appraising performance of a method by using a known dataset (a dataset with known anomaly and background samples). The results of the 3D U-statistics and concentration volume fractal are assumed as the real and correct thresholds (real

data) and so the misclassification errors of the Fibonacci-Transformation method could be estimated. The results of e_1 and e_2 estimations are shown in table 4.

Table 4. Misclassification errors of Fibonacci Transformation

	Error	In comparison to C-V fractal	In comparison to U-statistics
Background separation	e_1	0.13	0.03
	e_2	0	0
Moderate anomaly separation	e_1	0.01	0
	e_2	0	0.01
Strong anomaly separation	e_1	0.07	0.03
	e_2	0	0

The results of error estimations show that the Fibonacci Transformation method performs very well with an average total error of 0.023. This method in background and absolute anomalies detecting, performs more similar to U-statistics method while for moderate threshold recognition has more tendency to concentration volume fractal. The C-V fractal modeling calculates the volume based on the grade cutoff so the result is not sensitive to the location of samples while the U value in U-statistics method is devoted to the samples not only based on the variable value but also in accordance to the location of the sample. So, in case of absolute anomaly separating, higher regularity and less dispersion is achieved by U-statistics in comparison to C-V fractal modeling. This difference makes U-statistics method more reliable in detection of absolute anomalies.

This method uses cumulative values of a transformed variable for intervals that are defined by means of the Fibonacci sequence. This technique induces the feature of the Fibonacci numbers to the dataset only if the dataset follows Fibonacci features intrinsically. The FI ($FI = \frac{FibStdev}{Stdev}$) is an index or criterion to recognize such feature. Since the Fibonacci feature is a naturally created feature, variables with more correlation are expected to have closer Fibonacci indexes in multi-elemental datasets. Because the relation between different elements in exploration areas depends on the mineralization type and geological processes, the correlations between elements are interpreted and linked to the genetic of the mineralization. Based on this approach and referring to this fact that Fibonacci feature occurrence is a natural phenomenon, it is expected to see similar Fibonacci indexes for highly correlated elements.

In order to evaluate this assumption, Fibonacci indexes (FI) of 10 elements in our dataset were plotted with their correlation scores with gold (Au) (Figure 15). The correlation scores and FI values in figure 15 testify that the assumption was true and elements with higher correlation scores between them would have closer FI values too. This observation allows us to interpret Fibonacci features to investigate mineralization and geological processes too. Since it is the beginning of the way, more detailed studies are expected to take place in near future.

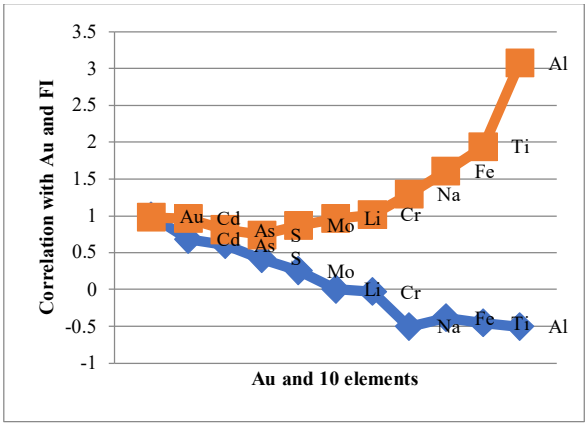


Figure 15. Correlation scores of 10 elements with Au and their FI values

4. Conclusions

One of the key steps of explorational geochemistry is separating anomalies from background. For aiming this goal, several types of methods are available in literature. These methods, especially the statistic approaches, do not consider the intrinsic features of geochemical datasets beyond the statistics. In other words, these methods were firstly designed for numerical calculations and statistical studies and then have been used by mining experts as tools for anomaly detection. Fibonacci features are intrinsic features that are seen in many natural phenomena and processes and the existence of Fibonacci ratios among many naturally grown flower components to even human body parts have been observed and proved. These

features have been introduced in this study for the first time as a possible feature of geochemical datasets. To evaluate this claim, a procedure named as Fibonacci Transformation method was established in this study. Based on the ratios among the well-known Fibonacci sequence numbers and the cumulative sum of the values of the favorable variable (gold in this study) this new method was introduced and evaluated by comparison to U-statistics and C-V fractal modeling.

The comparison of the results for anomaly detection (ore shape) revealed very high consistency between the results of the new method and the results obtained from U-statistics. The U-statistics is a robust structural approach that overcomes the challenges of anomaly detection in complex geological settings. The results of the Fibonacci Transformation method and U-statistics are in very high correlation in delimiting the background and strong anomaly thresholds. The concentration volume fractal and the Fibonacci Transformation methods surprisingly revealed almost the same results for moderate anomaly threshold (169ppb and 170ppb for gold respectively). To evaluate the overall performance of the Fibonacci method, the average total misclassification error was calculated and the outcome was 0.023 which is acceptable and quite reasonable since the methods are fundamentally different.

The second Fibonacci feature, $FI \leq 1$, is defined to determine dataset's Fibonacci feature. Datasets with $FI \geq 1$ do not contain Fibonacci characteristics and as a result the method should not be applied for them. The comparison of FI for different elements in the dataset of this study exhibits that element pairs with higher correlation scores do have closer FI values for the elements. This means that as long as the experts utilize correlation coefficient as a genetic factor for geochemical studies and ore evolution researches, they could use FI factor for the same purpose with this difference that FI comes from the natural features of the dataset and is not just a statistical measurement.

Appendix

"fibo_data_mining.m", Mendeley Data, V1, doi: 10.17632/sxbnxm4tt9.1

Refferences

[1]. Liu, Y., Zhou, K., & Cheng, Q. (2017). A new method for geochemical anomaly separation based on the distribution patterns of singularity indices. *Computers & Geosciences, 135*, 139–147.

[2]. Carranza, E. J. M. (2010). Catchment basin modelling of stream sediment anomalies revisited: Incorporation of EDA and fractal analysis. *Geochemistry: Exploration, Environment, Analysis, 10*(4), 365–381.

[3]. Carranza, E. J. M. (2011). Analysis and mapping of geochemical anomalies using logratio transformed stream sediment data with censored values. *Journal of Geochemical Exploration, 110*, 167–185.

[4]. Stanley, C. R., & Sinclair, A. J. (1987). Anomaly recognition for multi-element geochemical data: A background characterization approach. *Journal of Geochemical Exploration, 29*(1–3), 333–353.

[5]. Nazarpour, A., Paydar, G. R., & Carranza, E. J. M. (2016). Stepwise regression for recognition of geochemical anomalies: Case study in Takab area, NW Iran. *Journal of Geochemical Exploration, 168*, 150–162.

[6]. Gonbadi, A. G., Tabatabaei, S. H., & Carranza, E. J. M. (2015). Supervised geochemical anomaly detection by pattern recognition. *Journal of Geochemical Exploration, 157*, 81–91.

[7]. Liu, Y., Cheng, Q., Xia, Q., & Wang, X. (2014). Multivariate analysis of stream sediment data from Nanling metallogenic belt, South China. *Geochemistry: Exploration, Environment, Analysis, 14*(4), 331–340.

[8]. Yousefi, M., Kamkar-Rouhani, A., & Carranza, E. J. M. (2012). Geochemical mineralization probability index (GMPI): A new approach to generate enhanced stream sediment geochemical evidential map for increasing probability of success in mineral potential mapping. *Journal of Geochemical Exploration, 115*, 24–35.

[9]. Yousefi, M., Carranza, E. J. M., & Kamkar-Rouhani, A. (2013). Weighted drainage catchment basin mapping of geochemical anomalies using stream sediment data for mineral potential modeling. *Journal of Geochemical Exploration, 128*, 88–96.

[10]. Yousefi, M., Kamkar-Rouhani, A., & Carranza, E. J. M. (2014). Application of staged factor analysis and logistic function to create a fuzzy stream sediment geochemical evidence layer for mineral prospectivity mapping. *Geochemistry: Exploration, Environment, Analysis, 14*(1), 45–58.

[11]. Parsa, M., Maghsoudi, A., Yousefi, M., & Carranza, E. J. M. (2016). Multifractal interpolation and spectrum–area fractal modeling of stream sediment geochemical data: Implications for mapping exploration targets. *Journal of African Earth Sciences, 124*, 85–94.

[12]. Luz, F., Mateus, A., Matos, J. X., & Gonçalves, M. A. (2014). Cu- and Zn-soil anomalies in the NE border of the South Portuguese Zone (Iberian Variscides, Portugal) identified by multifractal and geostatistical analyses. *Natural Resources Research, 23*, 195–215.

[13]. Agterberg, F. P. (2014). *Geomathematics: Theoretical foundations, applications and future developments* (Vol. 18). Springer.

[14]. Afzal, P., Harati, H., Alghalandis, Y. F., & Yasrebi, A. B. (2013). Application of spectrum–area fractal model to identify geochemical anomalies based on soil data in Kahang porphyry-type Cu deposit, Iran. *Chemie der Erde – Geochemistry, 73*(4), 533–543.

[15]. Arias, M., Gumiel, P., & Martín-Izard, A. (2012). Multifractal analysis of geochemical anomalies: A tool for assessing prospectivity at the SE border of the Ossa Morena Zone, Variscan Massif (Spain). *Journal of Geochemical Exploration, 122*, 101–112.

[16]. Cheng, Q. (2007). Mapping singularities with stream sediment geochemical data for prediction of undiscovered mineral deposits in Gejiu, Yunnan Province, China. *Ore Geology Reviews, 32*(1–2), 314–324.

[17]. Cheng, Q. (1999). Spatial and scaling modelling for geochemical anomaly separation. *Journal of Geochemical Exploration, 65*(3), 175–194.

[18]. Cheng, Q., Xu, Y., & Grunsky, E. (2000). Integrated spatial and spectrum method for geochemical anomaly separation. *Natural Resources Research, 9*(1), 43–52.

[19]. Mokhtari, Z., & Sadeghi, B. (2021). Geochemical anomaly definition using multifractal modeling, validated by geological field observations: Siah Jangal area, SE Iran. *Geochemistry, 81*(4), 125774.

[20]. Shahbazi, S., Ghaderi, M., & Afzal, P. (2021). Prognosis of gold mineralization phases by multifractal modeling in the Zehabad epithermal deposit, NW Iran. *Iranian Journal of Earth Sciences, 13*, 31–40.

[21]. Chen, Y., Zhao, Q., & Lu, L. (2021). Combining the outputs of various k-nearest neighbor anomaly detectors to form a robust ensemble model for high-dimensional geochemical anomaly detection. *Journal of Geochemical Exploration, 231*, 106875.

[22]. Zuo, R., Wang, J., Xiong, Y., & Wang, Z. (2021). The processing methods of geochemical exploration data: Past, present, and future. *Applied Geochemistry, 132*, 105072.

[23]. Farhadi, S., Afzal, P., Boveiri Konari, M., Daneshvar Saein, L., & Sadeghi, B. (2022). Combination of machine learning algorithms with concentration-area fractal method for soil geochemical anomaly detection in sediment-hosted Irankuh Pb–Zn deposit, Central Iran. *Minerals, 12*(5), 689.

[24]. Tukey, J. W. (1977). *Exploratory data analysis*. Addison-Wesley.

[25]. Sinclair, A. J. (1974). Selection of threshold values in geochemical data using probability graphs. *Journal of Geochemical Exploration, 3*(2), 129–149.

[26]. Hawkes, H. E., & Webb, J. S. (1962). *Geochemistry in mineral exploration*. Harper and Row.

[27]. Xiao, F., Wang, K., Hou, W., & Erten, O. (2020). Identifying geochemical anomaly through spatially anisotropic singularity mapping: A case study from silver-gold deposit in Pangxidong district, SE China. *Journal of Geochemical Exploration, 210*, 106453.

[28]. Yang, Y., Yang, X., He, M., & Christakos, G. (2020). Beyond mere pollution source identification: Determination of land covers emitting soil heavy metals by combining PCA/APCS, GeoDetector and GIS analysis. *Catena, 185*, 104297.

[29]. Anaman, R., Peng, C., Jiang, Z., Liu, X., Zhou, Z., Guo, Z., & Xiao, X. (2022). Identifying sources and transport routes of heavy metals in soil with different land uses around a smelting site by GIS-based PCA and PMF. *Science of The Total Environment, 837*, 153759.

[30]. Salimi, A., Barak, S., & Yousefi, M. (2024). Using U-spatial statistics method to identify and classify intensity of geochemical anomalies in the Neysian area. *Scientific Quarterly Journal of Geosciences, 34*(3), 63–74.

[31]. Mohammadi, N. M., Hezarkhani, A., & Saljooghi, B. S. (2016). Separation of a geochemical anomaly from background by fractal and U-statistic methods: A case study from Khooni district, Central Iran. *Geochemistry, 76*(4), 491–499.

[32]. Matheron, G. (1962). *Traité de géostatistique appliquée* (Vol. 1). Editions Technip.

[33]. Yang, Z., Hu, G. D., Mei, H. B., & Yang, M. G. (2013). Application of residual anomaly component factor analysis method to the extraction of geochemical anomaly information from Gejiu western area. *Geological Science and Technology Information, 32*(6), 36–41. *(in Chinese with English abstract)*

[34]. Mandelbrot, B. B. (1983). *The fractal geometry of nature*. W.H. Freeman.

[35]. Yasrebi, A. B., Wetherelt, A., Foster, P., Coggan, J., Afzal, P., Agterberg, F., & Ahangaran, D. K. (2014). Application of a density-volume fractal model for rock characterization of the Kahang porphyry deposit. *International Journal of Rock Mechanics and Mining Sciences, 66*, 188–193.

[36]. Zhang, C., Zuo, R., & Xiong, Y. (2021). Detection of the multivariate geochemical anomalies associated with mineralization using a deep convolutional neural network and a pixel-pair feature method. *Applied Geochemistry, 130*, 104994.

[37]. Wang, H., Yuan, Z., Cheng, Q., Zhang, S., & Sadeghi, B. (2022). Geochemical anomaly definition using stream sediments landscape modeling. *Ore Geology Reviews, 142*, 104715.

[38]. Cheng, Q., Agterberg, F. P., & Ballantyne, S. B. (1994). The separation of geochemical anomalies from

background by fractal methods. *Journal of Geochemical Exploration, 51*(2), 109–130.

[39]. Afzal, P., Alghalandis, Y. F., Khakzad, A., Moarefvand, P., & Omran, N. R. (2011). Delineation of mineralization zones in porphyry Cu deposits by fractal concentration-volume modeling. *Journal of Geochemical Exploration, 108*(3), 220–232.

[40]. Sadeghi, B. (2021). Concentration–concentration fractal modelling: A novel insight for correlation between variables in response to changes in the underlying controlling geological–geochemical processes. *Ore Geology Reviews, 128*, 103875.

[41]. Gumiel, P., Sanderson, D. J., Arias, M., Roberts, S., & Martín-Izard, A. (2010). Analysis of the fractal clustering of ore deposits in the Spanish Iberian Pyrite Belt. *Ore Geology Reviews, 38*(4), 307–318.

[42]. Khalajmasoumi, M., Lotfi, M., Memar Kochebagh, A., Khakzad, A., Afzal, P., Sadeghi, B., & Ziazarifi, A. (2015). Delineation of the radioactive elements based on the radiometric data using concentration–area fractal method in the Saghand area, Central Iran. *Arabian Journal of Geosciences, 8*, 6047–6062.

[43]. Mokhtari, Z., Boomeri, M., & Bagheri, S. (2015). Application of multifractal modeling technique in systematic lithogeochemical survey to identify Au–Cu anomalies in the Siah Jangal area, Southeastern Iran. *Arabian Journal of Geosciences, 8*, 9517–9530.

[44]. Daneshvar Saein, L., & Afzal, P. (2017). Correlation between Mo mineralization and faults using geostatistical and fractal modeling in porphyry deposits of Kerman Magmatic Belt, SE Iran. *Journal of Geochemical Exploration, 181*, 333–343.

[45]. Ahmadfaraj, M., Mirmohammadi, M., Afzal, P., Yasrebi, A. B., & Carranza, E. J. M. (2019). Fractal modeling and Fry analysis of the relationship between structures and Cu mineralization in Saveh region, Central Iran. *Ore Geology Reviews, 107*, 172–185.

[46]. Mahdiyanfar, H., & Seyedrahimi-Niaraq, M. (2023). Integration of fractal and multivariate principal component models for separating Pb–Zn mineral contaminated areas. *Journal of Mining and Environment, 14*(3), 1019–1035.

[47]. Zuo, R. G., Xiong, Y. H., Wang, J., & Carranza, E. J. M. (2019). Deep learning and its application in geochemical mapping. *Earth-Science Reviews, 192*, 1–14.

[48]. Li, T. F., Xia, Q. L., Ouyang, Y. P., Zeng, R. L., Liu, Q. K., Chen, Y., & Li, T. T. (2024). Identifying geochemical anomalies associated with tungsten polymetallic mineralization using geographical detector and unsupervised machine learning methods: Application to the Nanling metallogenic belt, China. *Geochemistry, 84*, 126209.

[49]. Chen, Y., & Wu, W. (2017). Application of one-class support vector machine to quickly identify multivariate anomalies from geochemical exploration data. *Geochemistry: Exploration, Environment, Analysis, 17*, 231–238.

[50]. Moeini, H., & Torab, F. M. (2017). Comparing compositional multivariate outliers with autoencoder networks in anomaly detection at Hamich exploration area, east of Iran. *Journal of Geochemical Exploration, 180*, 15–23.

[51]. Esmaeiloghli, S., Lima, A., & Sadeghi, B. (2024). Lithium exploration targeting through robust variable selection and deep anomaly detection: An integrated application of sparse principal component analysis and stacked autoencoders. *Geochemistry, In Press*, 126111.

[52]. Guan, Q. F., Ren, S. L., Chen, L. R., Yao, Y., Hu, Y., Wang, R. F., Feng, B., Gu, L. D., & Chen, W. H. (2022). Recognizing multivariate geochemical anomalies related to mineralization by using deep unsupervised graph learning. *Natural Resources Research, 31*, 2225–2245.

[53]. Luo, Z. J., Zuo, R. G., Xiong, Y. H., & Wang, X. Q. (2021). Detection of geochemical anomalies related to mineralization using the GANomaly network. *Applied Geochemistry, 131*, 105043.

[54]. Zuo, R. G. (2017). Machine learning of mineralization-related geochemical anomalies: A review of potential methods. *Natural Resources Research, 26*, 457–464.

[55]. Onnis, L., & Carcione, J. M. (2017). A seismic ray tracing method based on Fibonacci search. *Annals of Geophysics, 60*(2), S0220.

[56]. Scott, T. C., & Marketos, P. (2014). On the origin of the Fibonacci sequence. *Presentation at Taiyuan University of Technology (TYUT)*.

[57]. Bonacci, L. (1202). *Liber Abbaci* (in Latin). Pisa.

[58]. Khachorncharoenkul, P., Phibul, K., & Laipaporn, K. (2022). The complex pulsating a1; a2; …; am, c) Fibonacci sequence. *Journal of King Saud University – Science, 34*(22), 102063.

[59]. Menhinick, C. N. (2015). *The Fibonacci resonance and other new golden ratio discoveries*. OnPerson International Limited.

[60]. Andrica, D. (2016). Book review. *Arab Journal of Mathematical Sciences*.

[61]. Cheddour, Z., Chillali, A., & Mouhib, A. (2023). Elliptic curve and k-Fibonacci-like sequence. *Scientific African, 20*, e01734.

[62]. Falcon, S., & Plaza, A. (2009). k-Fibonacci sequences modulo m. *Chaos, Solitons & Fractals, 41*(1), 497–504.

[63]. Edson, M., & Yayenie, O. (2009). A new generalization of Fibonacci sequences and extended Binet's formula. *Integers, 9*, 639–654.

[64]. Wall, D. D. (1960). Fibonacci series modulo m. *The American Mathematical Monthly, 67*(6), 525–532.

[65]. Deveci, O., & Shannon, A. G. (2018). The quaternion-Pell sequence. *Communications in Algebra, 46*(12), 5403–5409.

[66]. Sun, Z., et al. (2018). The mechanical principles behind the golden ratio distribution of veins in plant leaves. *Scientific Reports, 8*, 13859.

[67]. Douady, S., & Couder, Y. (1996). Phyllotaxis as a dynamical self-organizing process. *Journal of Theoretical Biology, 178*(3), 255–274.

[68]. Reimann, C., Filzmoser, P., & Garrett, R. G. (2002). Factor analysis applied to regional geochemical data: Problems and possibilities. *Applied Geochemistry, 17*(3), 185–206.

[69]. Zhao, J., Chen, S., & Zuo, R. (2016). Identifying geochemical anomalies associated with Au–Cu mineralization using multifractal and artificial neural network models in the Ningqiang district, Shaanxi, China. *Journal of Geochemical Exploration, 164*, 54–64.

[70]. Filzmoser, P., Hron, K., & Templ, M. (2018). Compositional data as a methodological concept. In *Applied Compositional Data Analysis* (pp. 1–16). Springer.

[71]. Filzmoser, P., & Hron, K. (2008). Outlier detection for compositional data using robust methods. *Mathematical Geosciences, 40*(3), 233–248.

[72]. Gott, J. R., & Colley, W. N. (2008). Median statistics in polling. *Mathematical and Computer Modelling, 48*(9–10), 1396–1408.

[73]. Gott, J. R., & Turner, E. L. (1977). Groups of galaxies. III. Mass-to-light ratios and crossing times. *Astrophysical Journal, 213*, 309–322.

[74]. Cheng, Q., Agterberg, F. P., & Bonham-Carter, G. F. (1996). A spatial analysis method for geochemical anomaly separation. *Journal of Geochemical Exploration, 56*(3), 183–195.

[75]. Ghavami-Riabi, R., Seyedrahimi-Niaraq, M., Khalokakaie, R., & Hazareh, M. (2010). U-spatial statistic data modeled on a probability diagram for investigation of mineralization phases and exploration of shear zone gold deposits. *Journal of Geochemical Exploration, 104*, 27–33.

[76]. Seyedrahimi-Niaraq, M. (2021). Comparison of U-spatial statistics method with classical statistics results in the determination of geochemical anomalies of epithermal gold in Khoshnameh area, Hashtjin, Iran. *Journal of Geological Research, 3*(2).

[77]. Ghannadpour, S. S., & Hezarkhani, A. (2016). Introducing 3D U-statistic method for separating anomaly from background in exploration geochemical data with associated software development. *Journal of Earth System Science, 125*(2), 387–401.

[78]. Agharezaei, M., & Hezarkhani, A. (2016). Delineation of geochemical anomalies based on Cu by the boxplot as an exploratory data analysis (EDA) method and concentration-volume (C–V) fractal modeling in Mesgaran mining area, Eastern Iran. *Open Journal of Geology, 6*(10), 1269–1278.

[79]. Tirrul, R., Bell, I. R., Griffis, R. J., & Camp, V. E. (1983). The Sistan suture zone of eastern Iran. *Geological Society of America Bulletin*.

[80]. Agharezaei, M., Hajari, H., & Hezarkhani, A. (2018). Qualitative contours: A new geochemical method for preliminary mineral exploration. *International Journal of Science and Engineering Applications, 7*, 08–19.

[81]. Sillitoe, R. H. (2010). Porphyry copper systems. *Economic Geology, 105*(1), 3–41.

[82]. Groves, D. I., & Bierlein, F. P. (2007). Geodynamic settings of mineral deposit systems. *Journal of the Geological Society, 164*(1), 19–30.

[83]. Bierlein, F. P., Murphy, F. C., Weinberg, R. F., & Lees, T. (2006). Distribution of orogenic gold deposits in relation to fault zones and gravity gradients: Targeting tools applied to the Eastern Goldfields, Yilgarn Craton, Western Australia. *Mineralium Deposita, 41*(1), 107–126.

[84]. Kerrich, R., Goldfarb, R. J., & Richards, J. P. (2005). Metallogenic provinces in an evolving geodynamic framework. In *100th Anniversary Volume* (pp. 1097–1136). *Economic Geology*.

[85]. Thompson, M., & Howarth, R. J. (1976). Duplicate analysis in geochemical practice. Part 1: Theoretical approach and estimation of analytical reproducibility. *The Analyst, 101*(1203), 690–698.

نشریه مهندسی معدن و محیط زیست
نشانی نشریه: www.jme.shahroodut.ac.ir
انجمن مهندسی معدن ایران
دانشگاه صنعتی شاهرود

معرفی روش تبدیل فیبوناچی برای جداسازی بخش‌های ناهنجار ژئوشیمیایی در مقیاس اکتشافات تکمیلی

محمدرضا آقارضائی، و اردشیر هزارخانی

دانشکده مهندسی معدن، دانشگاه صنعتی امیرکبیر، تهران، ایران

اطلاعات مقاله

تاریخ ارسال: ۲۰۲۵/۰۵/۱۸
تاریخ داوری: ۲۰۲۵/۰۶/۱۷
تاریخ پذیرش: ۲۰۲۵/۰۶/۱۸

DOI: 10.22044/jme.2025.16261.3157

کلمات کلیدی

تبدیل فیبوناچی
ویژگی‌های فیبوناچی
اندیس فیبوناچی
آنومالی ژئوشیمیایی

چکیده

ژئوشیمی اکتشافی به عنوان یک روش مفید اکتشافی، بیشتر به جدایش ناهنجاری و تلاش‌های مرتبط می‌پردازد. بسیاری از کارشناسان انواع مختلفی از روش‌های شناسایی ناهنجاری را پیشنهاد کرده‌اند. هدف این مطالعه معرفی یک روش جدید به منظور جداسازی ناهنجاری‌های ژئوشیمیایی بر اساس اعداد فیبوناچی برای اولین بار می‌باشد. ویژگی‌های فیبوناچی مجموعه داده‌ها شرح داده و روش معرفی شد و برای مطالعه یک مجموعه داده از نمونه‌های گمانه معدن طلای هیرد واقع در خراسان جنوبی به کار گرفته شد. نتیجه اصلی این مطالعه ایجاد موفق یک روش مبتنی بر اعداد فیبوناچی است که منجر به جداسازی ناهنجاری‌های ژئوشیمیایی می‌شود. حدود آستانه‌ای تعیین شده توسط این روش با آماره U و فرکتال عیار-حجم مقایسه شد. ارزیابی نتایج سازگاری بالایی بین خروجی حاصل از این روش‌ها را نشان می‌دهد. حد آستانه‌ای جدایش زمینه از ناهنجاری برای طلا توسط آماره U برابر با ۱۰۹ppb و توسط روش تبدیل فیبوناچی۱۰۵ ppb تعیین شد. این روش جدید برای ناهنجاری متوسط طلا حد آستانه‌ای ۱۷۰ppb را مشخص کرد که این عدد در روش فرکتال عیار-حجم ۱۶۹ppb تعیین شد که تقریبا برابر هستند. عملکرد این روش جدید با محاسبه خطای طبقه‌بندی مورد ارزیابی قرار گرفت. میانگین خطای طبقه‌بندی کل ۰.۰۲۳ بود که این عدد قابل قبول است و با توجه به این که روش‌ها به طور بنیادین متفاوت می‌باشند کاملا منطقی می‌باشد. به عنوان یکی دیگر از نتایج اصلی این روش، اثبات شد که یکی از ویژگی‌های فیبوناچی که تحت عنوان شاخص فیبوناچی (FI) تعریف شده، بین عناصر همان گونه نوسان می‌کند که ضریب همبستگی بین جفت عناصر عمل می‌کند. شاخص فیبوناچی می‌تواند به عنوان یک فاکتور ژنتیکی در مطالعات ژئوشیمیایی و تحقیقات تکامل منابع و ذخایر معدنی در نظر گرفته شود.

نویسنده مسئول مکاتبات: ardehez@aut.ac.ir (الف، هزارخانی)